

# PROGRESS IN COMPACT TOROID EXPERIMENTS

Thomas J. Dolan

Idaho National Engineering & Environmental Laboratory, USA, [dolatj@inel.gov](mailto:dolatj@inel.gov)

PACS: 52.55.Fa; 52.55.Ip; 52.55.Lf

## INTRODUCTION

The term “compact toroids” as used here means spherical tokamaks, spheromaks, and field reversed configurations, but not reversed field pinches. There are about 17 compact toroid experiments under construction or operating, with approximate parameters listed in Table 1.

Many of the experiments cited here are participating in a Coordinated Research Project of the International Atomic Energy Agency (IAEA) called “Comparison of Compact Toroid Configurations”. The goal is to foster international cooperation and to improve our

understanding of optimum plasma confinement in compact fusion devices.

## SPHERICAL TOKAMAKS (ST)

*MAST* [G. Counsell, A. Sykes, et al.]

The MegaAmpere Spherical Tokamak (MAST) at Culham Laboratory, UK, is shown in Figure 1. The MAST plasma energy confinement times agree with the international scaling IPB(y,2), with  $\tau_E$  values up to 100 ms in ELMy H-mode operation. There is good confinement in spite of (2,1) tearing mode activity and high frequency oscillations on soft x-rays from the plasma core. Values of  $\beta_N \sim 4.5$  and  $\beta_i \sim 15\%$  have been

Table 1. Approximate parameters of some compact toroid experiments. Parentheses indicate planned values.

	R / a, m	Ip, MA	B, T	Pulse, s	Heating, MW	Remarks
<b>Spherical Tokamaks</b>						
MAST, Culham	0.85/0.65	1.2 (2)	0.51	0.5 (5)	NBI = 2.5 (5) RF = 0.8 (1.5)	$n \sim 5 \times 10^{19} \text{ m}^{-3}$ $T_e \sim 1 \text{ keV}$ $\tau_E \sim 100 \text{ ms}$
NSTX, PPLL	0.85/0.68	1.4	0.45	0.5 (5)	NBI = 5 HHFW = 6	0.4 MW of CHI
TST-2, Tokyo University	0.38/0.25	0.12 (0.2)	0.2 (0.4)	0.02	HHFW = 0.1 (0.4)	
Globus-M, Ioffe Institute	0.37/0.24	0.25 (0.5)	0.35	0.06 (0.2)		
HIT, University of Washington	0.3/0.2	0.2	< 0.5	0.008	~ 10	Effects of voltage polarity
ETE, INPE, Brazil	0.3/0.2	0.2 (0.4)	0.4 (0.6)	0.01	(0.3)	$n \sim 1\text{--}(7) \times 10^{19} \text{ m}^{-3}$ $T_e = 100\text{--}(800) \text{ eV}$
SUNIST, Beijing	0.3/0.23	0.05	0.15		ECRH, FWCD	
Pegasus, Wisconsin	0.4/0.25	0.2	<0.2	0.03		
Proto-Sphera, Frascati, Italy	0.35/0.29	(0.12)		0.002	Cathode = 0.8	$(n \sim 10^{20} \text{ m}^{-3})$ $T \sim 130 \text{ eV}$
<b>Spheromaks</b>						
SSPX, LLNL, USA	0.31/0.26	0.6 (1.0)	0.25 (1)	0.004		$P_{\text{rad}}/P_{\text{in}} < 0.2$
UC Berkeley, USA			0.3	~ 0.0001	LHH = 20	
Unbounded spheromaks, Caltech, USA					Coaxial gun	Injected into large vacuum chamber.
<b>FRC</b>						
FIX, Osaka University			0.04		NBI = 0.6	$n = 5 \times 10^{19} \text{ m}^{-3}$ $T_e + T_i = 150 \text{ eV}$
TCS, Univ. of Washington	0.3/0.1	0.1	0.02	0.002	RMF = 3	Quasi-steady state, $n = 2 \times 10^{19} \text{ m}^{-3}$ , $T_e + T_i = 80 \text{ eV}$
TS-3, Tokyo Univ.	0.2/0.18		< 0.2			
TS-4, Tokyo Univ.	0.5/0.38	0.3	0.4			Spheromak, FRC, RFP, and ST.
Programming Compact Torus	0.15/0.15		0.5-2			Axial contraction → shock heating

observed, although no attempts have been made yet to probe the beta limit.

MAST can operate with a symmetric double null divertor (CDN), or with an asymmetric single-null divertor (SND) oriented upwards or downwards. Graphite tiles protect all plasma-facing surfaces. The H-mode is only observed near the CDN operation, which minimizes  $\delta r_{\text{sep}}$ , the distance between the inner and outer separatrices. Gas-puff fueling from the inboard side is more conducive to H-mode operation than outboard fueling. The MAST data extends the L-H transition power scaling information to higher values of inverse aspect ratio  $\epsilon$  and indicates that the required power increases roughly proportional to  $\epsilon^{1/2}$ .

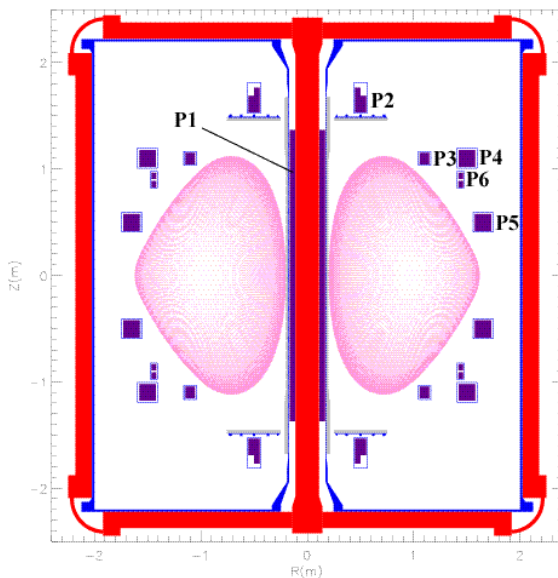


Fig. 1. The MAST toroidal field coils (rectangular), poloidal field coils, Ohmic heating coil, and plasma.

The ratio of L-mode power deposited on the outboard side to that on the inboard side is 10-30, with the higher values during edge localized modes (ELM) operation, and the lower values, between ELMs. The ELM frequency falls with increasing power to the scrape-off layer and rises with increasing electron density, which is consistent with “Type III” behavior. The highest confinement occurs at low ELM frequencies  $\sim 100$  Hz. The operation is near the ideal ballooning limit, where Type-I ELMs might be expected. A steep density gradient before the ELM collapses to a lower L-mode gradient after the ELM, with only a moderate change in the temperature profile. Energy losses are dominated by convection from the edge, with a strong correlation to the pedestal density. During ELMs the  $D_\alpha$  light emission zone extends over 10 cm outside of the separatrix.

During 2 MW of neutral beam injection (NBI) the peak heat flux reaches  $4 \text{ MW/m}^2$  on the outboard side. Application of 0-120 V toroidal bias potentials between 12 divertor segments induces ExB driven convective cells, which broaden the scrapeoff layer and reduce the power density. A new fast infrared camera will be used

to see how the power deposition shifts during biasing. The plasma detaches from the divertor in the L-mode at NBI power of 0.75 MW and core densities above  $3.5 \times 10^{19} \text{ m}^{-3}$ .

The “onion skin” code models quasi-single-null divertor plasma flows, for comparison with experimental data, such as reciprocating probe measurements of Mach numbers ( $M \sim 0.2$ ). It shows that magnetic mirror (grad-B) effects are important in the divertor region.

NSTX

[M. Peng]

The National Spherical Torus Experiment (NSTX, Figure 2) at Princeton Plasma Physics Laboratory and MAST both have similar dimensions, and both use carbon tiles to protect plasma-facing surfaces. However, NSTX has a close-fitting vacuum chamber for wall stabilization, while MAST has a very large chamber with internal magnetic field coils. NSTX can study coaxial helicity injection for plasma startup, while MAST can study “merging/compression”. Both use NBI heating. In addition, NSTX uses HHFW, while MAST uses ECRH.

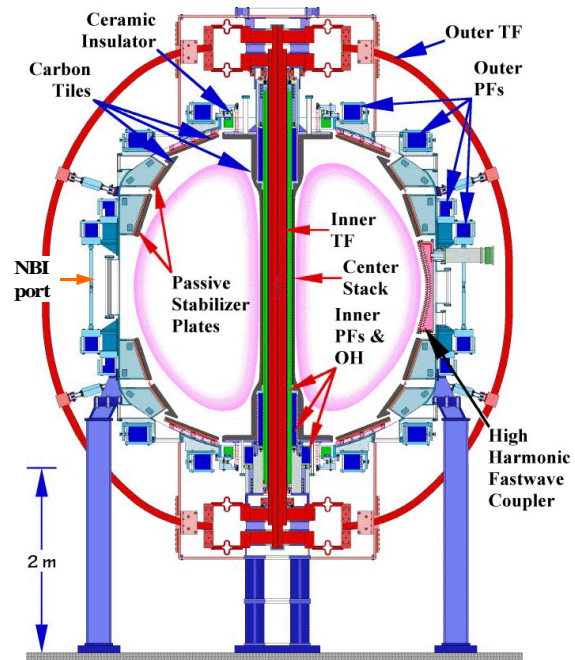


Fig. 2. The NSTX experiment.

In NSTX the high harmonic fast wave (HHFW) provides effective electron heating, increasing  $T_e$  from 0.4 keV to 0.9 keV. The electron density decreases  $< 10\%$  during HHFW heating. HHFW also interacts strongly with high energy ions, increasing the population of the high-energy tail ( $> 80$  keV).

Both NBI and HHFW can produce H-Mode plasmas. During NBI, confinement can reach H-Mode levels without observation of a distinct H-Mode transition. NBI produces high ion temperatures  $T_i \sim 2.5$  keV,  $T_e \sim 1.5$  keV and strong plasma rotation velocities  $\sim 200$  km/s. NBI fast ions excite magnetosonic oscillations, or compressional Alven Eigenmodes (CAEs).

Biased electrodes at the bottom of the torus produce coaxial helicity injection (CHI) current drive, which has induced up to 390 kA plasma current at CHI current

values < 30 kA. Magnetic and spectroscopic data are consistent with flux surface closure during CHI, but not yet conclusive. Success with CHI could lead towards solenoid-free startup in the future.

NSTX has achieved a “no-wall” limit of  $\beta_t \sim 25\%$  in L-mode plasmas without active control, and it aims to explore beta values up to 40%. The NSTX team is developing feedback control of error field response (amplified by strongly rotating high beta plasma) to raise beta.

Diagnostic probes are being added to look for the occurrence of sheared poloidal flow and radial streamers ( $\sim 10$  cm radially and  $\sim 10$  m along field lines) across the separatrix, which are predicted by computer simulations.

The potential advantages of spherical tokamaks include

- Solenoid-free startup and sustainment
- Reduced turbulence & improved confinement
- High toroidal beta
- Strong interaction of waves with energetic particles
- Dispersal of plasma heat flux over a large area.

The next step beyond NSTX could be a Performance Extension (PE) experiment with  $R \sim 1.5$  m,  $I_p \sim 5$  MA and pulse lengths > 10 s.

*TST-2* [Y. Takase]

The TST-2 spherical tokamak at the University of Tokyo is just starting HHFW heating experiments at a 100 kW power level. Electron temperatures in excess of 200 eV have been measured by a novel radio-reflectometer that measures EBW emission and mode conversion efficiency simultaneously. Ion temperature increases from a level of 100 eV to typically 500 eV at internal reconnection events.

*ETE* [G. Ludwig]

The Experimento Tokamak Esferico (ETE) in the Brazilian National Space Research Institute (INPE) will operate at  $B = 0.4$  T and  $I = 0.2$  MA with 10-15 ms pulse lengths. They will add 0.3 MW auxiliary heating. They implemented a Thomson scattering system with a 10 J, 20 ns Q-switched ruby laser, 5-channel polychromator filter, and avalanche photodiodes. The system will view 22 plasma positions along 50 cm of laser beam trajectory. They are developing 10 keV lithium neutral beam probe with a glassy beta-eucryptite source to study edge plasma density and fluctuations.

*Globus-M* [V. Gusev]

The Globus-M spherical tokamak at the Ioffe Institute, St. Petersburg, Russia, is in the early phases of operation. They have achieved a plasma current of 0.25 MA for 60 ms, which will be extended to 0.5 MA and 200 ms in the future.

*Helicity Injected Tokamak (HIT)* [T. Jarboe]

The HIT experiment injects helicity with injector current  $\sim 30$  kA and voltage = 300-600 V, depending on the polarity of the center column (higher voltages with negative center column) and achieves a plasma current  $\sim 200$  kA. Their analytic model explains the main features of CHI and MHD modes.

*PEGASUS* [R. Fonck]

The Pegasus tokamak, University of Wisconsin, has  $R/a = 1.1-2$ ,  $R = 0.2 - 0.45$  m,  $I \leq 0.45$  MA,  $B_t < 0.2$  T, and pulse length 20-40 ms. It can start up using the OH coil or an annular plasma gun. Its diagnostics include flux loops, Mirnov and Rogowski coils, soft x-ray pinhole monitors and camera, Ross filters, spectrometers, thermocouples, visible cameras, and bolometers, and a neutral beam probe is under development.

*SUNIST* [Y. X. He]

The Sino-United Spherical Tokamak (SUNIST) at Tsinghua University, Beijing, China, is nearing the end of construction. They will study ECRH startup, wave-plasma interaction, fast wave current drive, and possible operation without OH coils.

*Proto-Sphera* [F. Alladio]

The Proto-Sphera Tokamak at ENEA, Frascati, Italy, will replace the toroidal field coils with a 60 kA axial electron beam, Figure 3. The resulting toroidal field will be able to support a plasma current of 120 kA. It is anticipated that a plasma beta value of 20% will be stable. A ring of filamentary cathodes is under development to provide the electron beam.

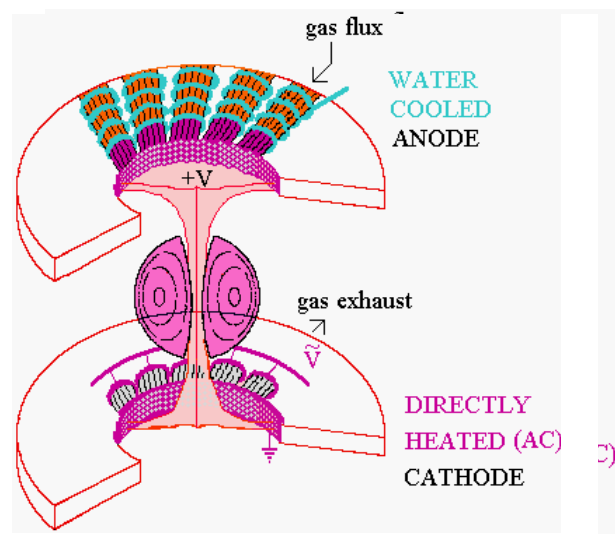


Fig. 3. The Proto-Sphera experiment.

## SPHEROMAKS

Spheromak plasmas can be produced by coaxial plasma guns or by magnetic flux cores. They have a natural stability by being near the Taylor minimum energy state, and only weak external magnetic fields are required, but the attainable plasma beta values are probably on the order of 10%.

*SSPX* [E.B. Hooper, D. Hill, et al.]

The Sustained Spheromak Physics Experiment (SSPX) at LLNL is shown in Figure 4. SSPX produces plasma by coaxial electrodes and drives the plasma into the flux conserver region, where it is sustained. The goal

of SSPX is to sustain a toroidal plasma current of 1 MA for 3 ms, with a corresponding magnetic field of 1 T. So far they have achieved a field of 0.2 T for 3 ms. The radiated power is less than 20% of the input power, which indicates a low level of impurity contamination. Magnetic fluctuation levels of  $\sim 1\%$  are obtained with electron temperatures  $> 150$  eV. Diagnostics include a multi-point Thomson scattering system, a transient internal probe, and an ultra-short-pulse reflectometer to measure  $n$  and  $B$ . The CORSICA code is used to analyze the surface magnetic probe data. The copper flux conserver is coated with tungsten to resist sputtering.

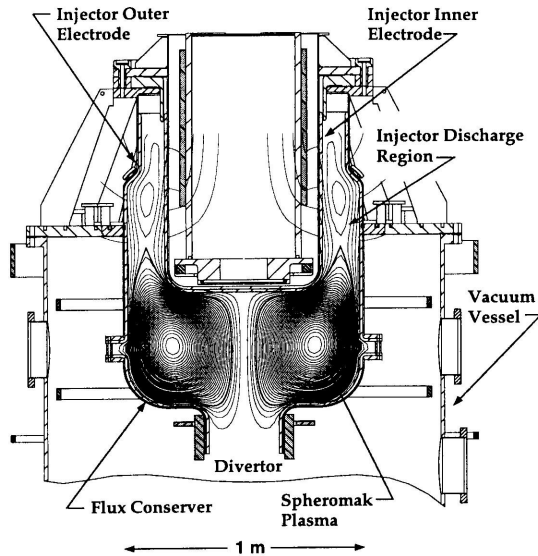


Fig. 4. The SSPX experiment.

*UC Berkeley Spheromak* [E. Morse]

The UC Berkeley Spheromak has  $B_{\text{pol}} \sim 0.3$  T,  $n \sim 5 \times 10^{20} \text{ m}^{-3}$ , and  $T_e \leq 150$  eV. It injects 20 MW of 450 MHz lower hybrid waves through a slot in the flux conserver. This RF power supply will also be loaned to the SSPX experiment. Diagnostics include Thomson scattering, a 3.8 m ion Doppler spectrometer, a HeNe interferometer, and magnetic probes. There is substantial MHD activity, and the plasma decays after 100  $\mu\text{s}$ .

*Unbounded spheromaks* [P. Bellan]

The California Institute of Technology injects unbounded spheromaks from a coaxial plasma gun into a large vacuum chamber and photographs them with a high-speed camera. The spheromaks are formed over a distinct range of  $\lambda$ , the ratio of gun current to gun bias flux. Immediately after formation the spheromaks flow away from the gun at a constant velocity and expand self-similarly. In the regime where  $\lambda$  is marginally insufficient to form spheromaks, helically twisted flux tubes, reminiscent of solar prominences, are observed.

The TST-3 and TST-4 devices, which also produce spheromak plasmas, will be discussed in the next section.

*RMS* [R. Bourque and P. Parks]

A Repetitively Merging Spheromak (RMS) reactor concept would shoot spheromaks axially at up to 1900 km/s into a central chamber at a rate of about 20 Hz. The central plasma toroidal current would gradually build up to 85 MA in about two hours. Then the plasma density would be increased to the desired level and fusion burn would generate 500 MWe. The plasma would be sustained indefinitely at 10% beta by continued spheromak injection, with about 8% recirculating power.

**FIELD REVERSED CONFIGURATIONS (FRC)**

A field reversed configuration (FRC) differs from a spheromak by having zero toroidal magnetic field. FRC plasmas are produced by programmed theta pinch devices, by merging two spheromaks with opposite toroidal fields, or by rotating magnetic field (RMF) current drive. They have experimental stability exceeding theoretical predictions, and they can in principle confine high-beta plasmas, but only modest experiments have been built, and experimentally observed confinement times have so far been short.

*TCS* [A. Hoffman]

Following the successful Rotamak experiment in Australia, the University of Washington is studying the use of RMF current drive to sustain FRC plasmas. The RMF drags the electrons like an induction motor, inducing a toroidal plasma current and poloidal magnetic field. The RMF initially penetrates into the plasma, then becomes partially excluded. A reduction of plasma resistivity would improve confinement. The LSX/Mod experiment uses a high voltage theta pinch to form the FRC, then moves it axially into the RMF chamber. FRCs can be formed by RMF alone, or formed in LSX/Mod and translated into TCS (Translation-Confinement-Sustainment), where they can be sustained by 3 MW RMF at 80 kHz. The data show that the internal magnetic field is in the opposite direction from the external magnetic field of the FRC. An uncontrolled increase of plasma density from ionization of neutral gas interferes with confinement. In the future they will use metal chamber walls and wall conditioning to sustain better plasma purity, to reduce gas influx and radiation losses, and to achieve higher electron temperature, hence longer confinement times.

*FIX* [S. Goto]

The FIX experiment at Osaka University also produces an FRC plasma ( $n = 5 \times 10^{21} \text{ m}^{-3}$ ,  $T_e + T_i = 400$  eV) with a theta pinch and translates it axially into a second chamber, where it reflects without significant losses from the mirror coil at the far end of the chamber, and expands to  $n = 5 \times 10^{19} \text{ m}^{-3}$ ,  $T_e + T_i = 150$  eV. Then NBI (0.6 MW at 15 keV) heats the plasma and partially sustains it. As a result, the confinement time increases from 95  $\mu\text{s}$  (no NBI) to 230  $\mu\text{s}$  (with NBI). RF power from a ringing capacitor bank at 100 kHz, coupled via a pair of azimuthal loop antennas that excite  $B_r$  and  $B_z$  wave fields, increases  $T_i$  by 25%, probably by excitation of a shear Alfvén wave.

TS-3 and TS-4

[Y. Ono]

The TS-3 device at the University of Tokyo has  $R \sim 0.2$  m,  $R/a \sim 1.05 - 2.0$ , and  $B < 0.2$  T, and coaxial plasma guns that can produce and collide two spheromak plasmas. If the colliding spheromaks have opposite  $B_t$ , then the toroidal field annihilates, producing ion heating and an FRC plasma with  $\beta \sim 70\%$ . The new TS-4 device, Figure 5, has  $R = 0.4 - 0.55$  m,  $R/a = 1.2 - 1.9$ ,  $B = 0.3 - 0.5$  T, and  $I_p = 300$  kA. TS-4 has both coaxial plasma guns and flux cores for producing spheromaks. It also has

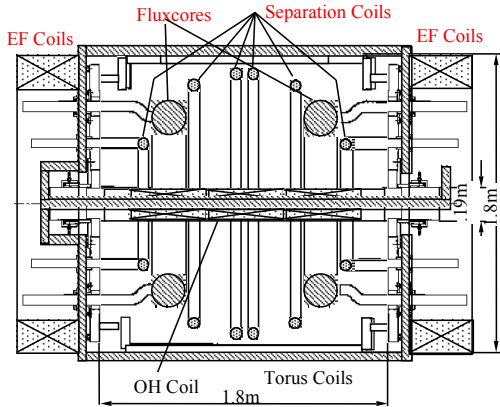


Fig. 5. The TS-4 Experiment.

a conducting rod along the axis to produce an optional toroidal magnetic field and to help stabilize the tilt instability. These TS-3 and TS-4 devices have the unique capability of producing spherical tokamaks, reversed field pinches (RFPs), spheromaks, and FRCs all in the same device, as shown in Figure 6.

Spherical tokamaks have  $q > 1$ , spheromaks have  $q \sim 0.5$ , FRCs have  $q \sim 0$ , and RFP have  $q \sim 0.3$ . The dominant dynamo mode of an RFP with  $R/a \sim 1.5$  is  $n=3$ , while that of a spheromak is  $n=2$ . Two spheromaks can be merged into an FRC, which is then transformed into a high-beta (50-70%) spherical tokamak by application of a toroidal magnetic field. The resultant spherical tokamak has an absolute minimum-B magnetic field topology, and it is in the second stability regime of the ballooning mode. The high-beta tokamak disrupts when its  $q$  profile enters the unstable regime. The flexible ST-3 and ST-4 devices can thus facilitate valuable comparisons of various plasma configurations.

Programming Compact Torus [R. Kurtmullaev]

The Programming Compact Torus device at TRINITY Laboratory, Troitsk, Russia, produces an FRC plasma with a programmed theta pinch coil. The plasma contracts axially at speeds  $> 10^5$  m/s, which results in adiabatic compression,  $B \sim 2$  T, and strong ion heating up to  $T_i \sim 3$  keV.

## STABILITY AND TRANSPORT

Spherical tokamaks can suffer disruptions, kinks, ballooning modes, neoclassical tearing, and resistive wall modes. Usually strong disruptions are not observed, but internal reconnection events with multiple high-mode-

number harmonics occur. Plasma shaping, profile

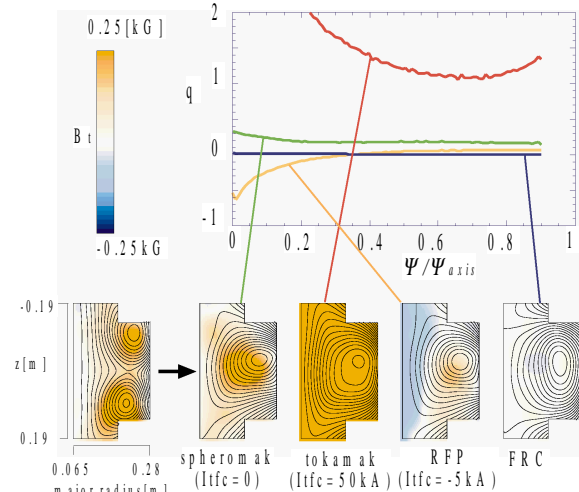


Figure 6. Various modes of TS-4 operation and  $q$  profiles.

control, and flow shear can help to stabilize the plasmas. Spheromaks can suffer from the tilt instability and relaxation events. Their stability can be aided by the Taylor minimum energy state, by energetic ions, by a flux conserver, by plasma rotation, and by finite Larmor radius effects. FRC plasmas are vulnerable to tilting and rotational modes and to plasma density buildup. Their stability, which appears to exceed simple theoretical expectations, is aided by plasma flow and finite Larmor radius effects.

Spherical tokamaks have attained H mode operation, with improved transport. Internal transport barriers may occur, and microturbulence may be suppressed by magnetic shear, flow shear, and in some cases by a magnetic well. Spheromaks have dynamo reconnection phenomena, which increases transport rates. Transport is improved in decaying, isolated spheromaks, and it should improve at higher  $T_e$ . There is a transport barrier only near the separatrix. Transport in FRCs is anomalous, and not well understood.

## SUMMARY

Compact toroid research underway in many countries is producing some interesting results, such as H-mode operation (spherical tokamaks), high beta, coaxial helicity injection, rotating magnetic field current drive, HHFW heating, and novel diagnostics, in spite of low budgets. If successful, compact toroids might facilitate fusion power at lower cost, with a variety of applications for electrical power production, materials testing, waste transmutation, hydrogen production, and space travel.

## ACKNOWLEDGEMENT

The following scientists generously provided information about their research: Paul Bellan, Robert Bourque, Glenn Counsell, Ricardo Farengo, Seichi Goto, David Hill, Alan Hoffman, Ed Morse, Rustam Kurtmullaev, Gerson Ludwig, Brian Nelson, Martin Peng, Yasushi Ono, Alan Sykes, and Yuichi Takase.

